THE JOURNAL OF BIOLOGICAL CHEMISTRY VOL. 281, NO. 36, pp. 26361–26369, September 8, 2006

Anti-hemostatic Effects of a Serpin from the Saliva of the Tick *Ixodes ricinus*[*]

Received for publication, May 2, 2006 Published, JBC Papers in Press, May 3, 2006, DOI 10.1074/jbc.M604197200

Pierre-Paul Prevot[‡], Benoit Adam[§1], Karim Zouaoui Boudjeltia[¶], Michel Brossard[‖], Laurence Lins[§], Philippe Cauchie[¶], Robert Brasseur[§], Michel Vanhaeverbeek[¶], Luc Vanhamme[**], and Edmond Godfroid[‡2]

From the Departments of [‡]Génétique Appliquée and [**]Parasitologie moléculaire, Institut de Biologie et de Médecine Moléculaires, Université Libre de Bruxelles, Rue des Professeurs Jeener et Brachet, 12, B-6041 Gosselies, Belgium, the [§]Centre de Biophysique Moléculaire et Numérique, Faculté Universitaire des Sciences Agronomiques de Gembloux, B-6110 Gembloux, Belgium, the [¶]Laboratoire de Médecine Expérimentale, Centre Hospitalier Universitaire André Vésale, Université Libre de Bruxelles, B-5030 Montigny-le-Tilleul, Belgium, and the [‖]Institut de Zoologie, Université de Neuchâtel, CH-2000 Neuchâtel, Switzerland

Serpins (serine protease inhibitors) are a large family of structurally related proteins found in a wide variety of organisms, including hematophagous arthropods. Protein analyses revealed that Iris, previously described as an immunomodulator secreted in the tick saliva, is related to the leukocyte elastase inhibitor and possesses serpin motifs, including the reactive center loop (RCL), which is involved in the interaction between serpins and serine proteases. Only serine proteases were inhibited by purified recombinant Iris (rIris), whereas mutants L339A and A332P were found devoid of any protease inhibitory activity. The highest K_a was observed with human leukocyte-elastase, suggesting that elastase-like proteases are the natural targets of Iris. In addition, mutation M340R completely changed both Iris substrate specificity and affinity. This likely identified Met-340 as amino acid P1 in the RCL. The effects of rIris and its mutants were also tested on primary hemostasis, blood clotting, and fibrinolysis. rIris increased platelet adhesion, the contact phase-activated pathway of coagulation, and fibrinolysis times in a dose-dependent manner, whereas rIris mutant L339A affected only platelet adhesion. Taken together, these results indicate that Iris disrupts coagulation and fibrinolysis via the anti-proteolytic RCL domain. One or more other domains could be responsible for primary hemostasis inhibition. To our knowledge, this is the first ectoparasite serpin that interferes with both hemostasis and the immune response.

Ticks are blood-sucking arthropods that infest a large variety of vertebrate hosts (mammals, birds, reptiles, and amphibians) in many parts of the world (1). To complete their blood meal, blood-sucking arthropods express a wide range of anti-hemostatic molecules in their saliva, including vasodilators, inhibitors of the platelet aggregation, and anti-coagulants (2). Tick saliva and salivary gland extracts are also known to modulate the host's defense mechanisms (3–6). Both anti-hemostatic and immunosuppressive compounds were identified, isolated, and characterized from soft and hard ticks. These compounds include histamine-binding proteins, tissue factor pathway inhibitor-like proteins, anti-thrombin-like proteins, and anti-complement factors (7–16).

These last years, several laboratories reported the construction and screening of cDNA libraries from tick salivary glands. Thus, Das *et al.* (17) found 14 *Ixodes scapularis* immunodominant antigens, whereas Leboulle *et al.* (18) identified 27 mRNA, the expression of which is specifically induced or up-regulated during the *Ixodes ricinus* blood meal. Finally, Ribeiro and co-workers explored the sialome of the tick *I. scapularis* (19, 20) and uncovered a large variety of putative bioactive agents. These studies all identified some serine protease inhibitors, containing serpin, kunitz, kazal, or α-macroglobulin motifs (21).

To date, ~500 serpins have been identified in a large variety of species, including animals, viruses, and plants. On average, serpins are 350–400 amino acids long. In human plasma, they make up ~2% of the total protein amount, of which 70% is α-1-antitrypsin. Both extracellular and intracellular serpins have been identified (22). Members of the superfamily of serine protease inhibitors are expressed in a cell-specific manner and are involved in a number of fundamental biological processes such as blood coagulation, complement activation, fibrinolysis, angiogenesis, inflammation, and tumor suppression (23–25). The protein structure of serpins is usually characterized by three β-sheets (A, B, and C) and eight or nine α-helices (26). A typical feature of serpins is the reactive center loop (RCL),[3] a protein motif composed of ~20 amino acids, located near the C terminus of the protein. This motif contains a scissile bond between residues called P1 and P1′, which is cleaved by the target protease. Once cleaved, the RCL domain traps the protease and moves to the opposite pole of the serpin through the β-sheet A. This tight association results in an irreversible loss of structure and distortion of both the protease and the serpin. Inside the RCL domain the hinge region (amino acids P15–P9)

[*] This work was supported in part by the Région Wallonne (Belgium) (Grants 215054, 215107, and 215370). The costs of publication of this article were defrayed in part by the payment of page charges. This article must therefore be hereby marked "*advertisement*" in accordance with 18 U.S.C. Section 1734 solely to indicate this fact.
[1] Supported by the Ministère de la Région Wallonne (Grant 215370).
[2] To whom correspondence should be addressed. Tel.: 32-2-650-9934; Fax: 32-2-650-9900; E-mail: Edmond.Godfroid@ulb.ac.be.

[3] The abbreviations used are: RCL, reactive center loop; HLE, human leukocyte elastase; Iris, *I. ricinus* immunosuppressor; PAI-1, plasminogen activator inhibitor, type 1; PDB, Protein Data Bank; PPE, pancreatic porcine elastase; RBD, rIris, recombinant Iris; r.m.s.d., root mean square deviation; t-PA, tissue plasminogen activator; HBSS, Hanks' balanced salt solution; ECLT, euglobulin clot lysis time; ANOVA, analysis of variance; MMP, metalloprotease; PFA, platelet function analyzer.

is implicated in the stabilization of the interaction with the protease and provides mobility for the integration of the RCL in β-sheet A. Some serpin family members, while structurally similar to inhibitor serpins, have no inhibitory functions. These non-inhibitory serpins include corticosteroid binding globulin and thyroxine binding globulin, which are involved in hormone transport, angiotensinogen, which is a peptide hormone precursor, and ovalbumin. These serpins retain the mobility of the RCL domain. However, there is no evidence for a conformational change following cleavage at their putative reactive centers.

A few serpins have been recently isolated from the hard ticks *Amblyomma hebraeum*, *Amblyomma variegatum*, *Boophilus microplus*, *Hemaphysalis longicornis*, *I. scapularis*, and *Rhipicephalus appendiculatus* (27–30). These proteins are mainly expressed in tick salivary glands and are secreted in the saliva. Most of them have been proposed as targets in an anti-tick mixture vaccine (30–32, 34).

Recently, we have characterized a protein, which is up-regulated during the blood meal and modulates both the innate and acquired immunity of the host (35). Accordingly, we named the protein Iris for "*I. ricinus* immunosuppressor." Iris was also found to be related to the pig leukocyte elastase inhibitor (35). In this report, we present the cloning and the expression of Iris as well as single point mutants in insect cells. Structural analysis and directed mutagenesis confirmed that Iris is a serpin with Met-340 as the P1 residue. We also show that Iris is a specific elastase inhibitor that interferes with the coagulation pathways and the fibrinolysis process via the RCL domain. Finally, we show that Iris inhibits platelet adhesion via another functional domain. To our knowledge, this is the first ectoparasite serpin that alters both hemostasis and the immune response.

MATERIALS AND METHODS

Plasmid Construction, Protein Expression, and Purification—The coding sequence for Iris (formerly Seq24; accession number AJ269658) was subcloned from vector pCDNA3.1-V5-His/Iris (35) between the KpnI/AgeI restriction sites of vector pBlueBac4.5-V5-His (Invitrogen) in-frame with the coding sequence of the V5 and His epitopes at the C terminus. Recombinant baculoviruses were made by recombination between pBlueBac/Iris and Bac-N-Blue linear DNA virus (Invitrogen). Recombinant viruses were selected and amplified according to the manufacturer's instruction. SF9 cells were infected with a high titer stock of recombinant baculovirus and were incubated for 55 h at 27 °C. Cells were then lysed using the French press, and spun at $10^6 \times g$ for 40 min. The recombinant protein was further purified in one step from the cleared supernatant by chelating chromatography over Ni^{2+}-Sepharose (Qiagen). Recombinant Iris was eluted in 50 mM Tris-HCl (pH 7.5) containing 500 mM NaCl and 150 mM imidazole. All purification steps were carried out at 4 °C. Typically, 50 mg of purified rIris was obtained per liter of suspension culture.

Site-directed Mutagenesis of Iris in pBlueBac4.5 V5 His—Mutants were produce by using the QuikChange PCR mutagenesis kit (Stratagene). The following PCR primers were used to generate P9, P2, and P1 mutants, respectively: 5′-GCA CAG AGG CTG CAG CTC CCA CTG CCA TAC CC-3′ (forward A332P), 5′-GGG TAT GGC AGT GGG AGC TGC AGC CTC TGT GC-3′ (reverse A332P); 5′-GCC ATA CCC ATT ATG GCG ATG TGC GCG AGA TTT CC-3′ (forward L339A), 5′-GGA AAT CTC GCG CAC ATC GCC ATA ATG GGT ATG GC-3′ (reverse L339A); 5′-GCC ATA CCC ATT ATG TTG CGG TGC GCG AGA TTT CC-3′ (forward M340R), 5′-GGA AAT CTC GCG CAC CGC AAC ATA ATG GGT ATG GC-3′ (reverse M340R); where the underlined nucleotides generate the mutation. Supercompetent XL1-Blue cells were transformed according to the manufacturer's instructions, and the plasmids were purified to confirm the sequence modifications by sequencing.

Molecular Modeling—Three-dimensional models of Iris were generated using the homology modeling software Modeler 6.2 (36). To construct a model, the sequence of Iris was aligned to a homologous sequence whose three-dimensional structure had been experimentally determined. For that purpose, the Protein Data Bank (PDB) was screened using the Blast algorithm. α-Antitrypsin (PDB code: 1ATU) was selected as the template for the native model and horse leukocyte elastase inhibitor (PDB code: 1HLE) for the cleaved model. The percentages of identity with Iris are 32 and 42%, respectively, and the percentages of similarity 51 and 59%, respectively. To further examine the homology, the hydrophobic cluster analysis plots of both sequences were compared. Briefly, the hydrophobic cluster analysis method is based on a two-dimensional helical plot of the sequence and allows detection of hydrophobic clusters in proteins (37). The stereochemical quality of the minimized three-dimensional model was assessed using Procheck (38). Both models had no residues located in the disallowed regions of the Φ, Ψ angle pairs of the Ramachandran plot, indicating correct stereochemistry. Molecular views were drawn with WinMGM (39).

A model of the interaction between Iris and a protease was built using Swissmodel (40). The template was the complex between trypsin and alaserpin A353K (PDB code: 1K9O). The Pex algorithm was used to analyze the residues in this interaction. This method extracts numeric and string descriptions of protein structures from PDB files and lists parameters such as the dihedral angles, the N–H bond lengths, the secondary structure, the closest residues in the interaction, and the minimal distance of the interaction (41).

Enzymatic Assays—To assay the inhibition of proteases, Iris was mixed in a microcuvette with 5–20 μl of a protease at an equimolecular ratio in 50 mM Tris-HCl (pH 7.5) containing 100 mM NaCl. Residual activity was measured by adding 1 ml of 0.5 mM of an appropriate chromogenic substrate in 50 mM Tris-HCl, pH 7.5, 100 mM NaCl. The increase in absorbance at 405 nm over time was measured. Two variants of the assay were performed: (i) in a first, residual activity was measured after incubation for 1 h at 37 °C, (ii) in a second, activity was measured as function of the incubation time. In the former case, residual activity in the presence of ovalbumin, which is a serpin with no inhibitory activity, was taken as the 100% reference point. rIris was tested in the presence of the following subset of enzyme-substrate systems: human thrombin and *N*-benzoyl-Phe-Val-Arg-*p*-Na; human leukocyte elastase (HLE) and *N*-(methoxysuccinyl)-Ala-Ala-Pro-Val-*p*-Na; porcine pancreatic elastase (PPE, Roche Applied

Science), and *N*-methoxysuccinyl-Ala-Ala-Pro-Val-*p*-Na; human plasmin and *N*-*p*-tosyl-Gly-Pro-Lys-*p*-Na; human factor Xa and factor Xa chromogenic substrate; recombinant tissue plasminogen activator (t-PA, Hyphen Biomed, France) and t-PA chromogenic substrate; and human trypsin and *N*-benzoyl-Phe-Val-Arg-*p*-Na. We also tested two cysteine proteases (papain with pGlu-Phe-Leu-*p*-Na and caspase 3 with *N*-acetyl-Asp-Glu-Val-Asp-*p*-Na) and one human metalloelastase (MMP12 with MMP chromogenic substrate, Biomol). All products were purchased from Sigma-Aldrich, unless otherwise indicated.

Measurement of Association Rate Constants—The association rate constant (k_a) describes the inhibition kinetics of free serine proteases by serpins. It was determined by mixing proteases and rIris for variable periods of time before addition of the substrate (0.5 mM), which slows down the association process enough to allow measurement of residual enzyme activity (42). Considering that the dissociation reaction is slow with respect to the interval of time needed to follow association, the rate association, $-d[E]/dt$ is given by Equation 1 (42).

$$-\frac{d[E]}{dt} = k_a \cdot [E][I] \qquad \text{(Eq. 1)}$$

The rate of association was either under second order conditions ($[E]_0 = [I]_0$) or pseudo-first order conditions ($[I]_0 > 10[E]_0$). In the former case, non-linear regression analysis was used to fit the data to the following second-order equation,

$$[E] = \frac{[E]_0}{(1 + [E]_0 \cdot k_a \cdot t)} \qquad \text{(Eq. 2)}$$

where E is the concentration of free enzyme at any time, t, and E_0 is the concentration at $t = 0$. E_0 and E are proportional to the rate of substrate hydrolysis at $t = 0$ and at any time, respectively.

When pseudo-first order rate constants were used, the data were fitted to the following exponential equation,

$$[E] = [E]_0 \cdot e^{-k_a \cdot [I]_0 \cdot t} \qquad \text{(Eq. 3)}$$

where I_0 is the I concentration at $t = 0$.

Clotting Assays—The tests were performed on a pool of citrated platelet-poor human plasma from six healthy, fully informed, and consenting adult volunteers. Aliquots were stored at −80 °C until analysis. Recombinant Iris was dialyzed in phosphate-buffered saline devoid of Ca^{2+} and Mg^{2+}. The effects of 1.5–6 μM rIris on coagulation time were evaluated on BCT machine (Dade, Behring). Phospholipids and activators (Innovin 1/200 for tissue factor, PTT 1/4 for contact phase activation) were added to 50 μl of spiked plasma. Clotting time was recorded after the addition of 50 μl of 25 mM $CaCl_2$.

Cell-based clotting time assays were performed by adding 6 μM rIris to a mixture of human plasma and the human monocytes THP1 (10^6 cells/ml final). The mix was then incubated at 37 °C for 5 min. Clotting times were measured after addition of 100 μl of 25 mM $CaCl_2$.

Euglobulin Clot Lysis Time—The euglobulin fraction was prepared as described by Zouaoui Boudjeltia *et al.* (43). Briefly, 300 μl of acetic acid (0.025%) and 3.6 ml of deionized water were added to 400 μl of pooled human plasma. The

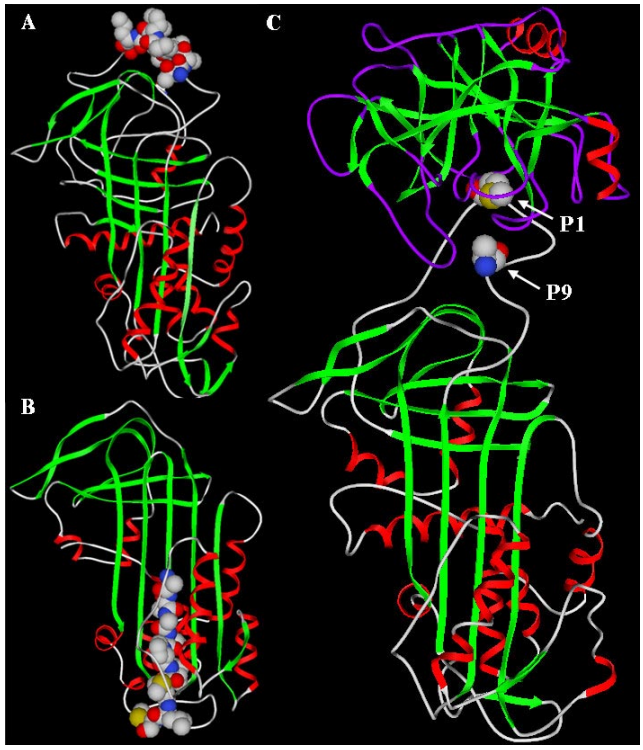

FIGURE 1. **Three-dimensional models of Iris.** Three-dimensional structures of Iris were constructed by homology modeling using as templates homologous proteins uncovered by Protein Data Bank screening. *A*, uncleaved model based on the structure of α-antitrypsin (PDB code: 1ATU), which shares 32% identity with Iris. *B*, cleaved model based on the structure of horse leukocyte elastase inhibitor (PDB code: 1HLE), which shares 40% identity with Iris. *C*, model of the interaction based on the structural model of the trypsin-alaserpin interaction (33% identity with Iris). β-Sheets are in *green*; α-helices are in *red*; coil structures are in *white* for Iris and in *purple* for trypsin.

sample was centrifuged at $4.0 \times 10^3 \times g$ for 10 min at 4 °C. The supernatant was discarded, and the pellet was resuspended in 400 μl of Hanks' balanced salt solution (HBSS) containing increasing concentrations of rIris, with or without added neutrophils (final concentration 5×10^6 per ml). Clot formation was started by adding 100 μl (1.5 units/ml) of thrombin. ECLT was measured by a semi-automatic method using a "Lysis Timer" device (43).

In addition, another test was performed to exclude the effects of the interaction of Iris on the cell surface. Cells were incubated with rIris for 1 h and then washed three times in phosphate-buffered saline. Washed cells were then resuspended in HBSS before use in the ECLT test.

Primary Hemostasis—Blood samples were collected from five healthy, fully informed, and consenting volunteers in 0.13 M citrate vacuum tubes. Global platelet function was measured on PFA-100® machine (Dade, Behring) with the collagen/epinephrine cartridge. This apparatus creates an artificial vessel consisting of a bioactive membrane with a microscopic aperture (44). The sample (1/10 protein in HBSS and 9/10 anti-coagulated whole blood) was aspirated through a capillary under steady high shear rates (5000 – 6000 s^{-1}) within 2 h of sample collection. The presence of the platelet agonist and the high shear rates result in a platelet plug that gradually occludes the aperture. The closure time is considered to be the time required to obtain full occlusion of the aperture.

Statistical Analyses—SigmaStat® software (Jandel Scientific, Erkrath, Germany) was used for the analysis. Data are represented as mean ± S.D. and were evaluated by one-way ANOVA. The effect of rIris on platelet adhesion was evaluated by a Friedman repeated measures analysis of variance on ranks test.

RESULTS

Molecular Modeling—Iris had previously been found to be similar to the pig leukocyte elastase inhibitor (35). In addition, membership in the serpin superfamily was confirmed by the high conservation of consensus residues identified by Irving and colleagues (45). All conserved residues among serpins are also conserved in Iris except for the replacement of Phe-106 by Tyr, Ile-134 by Val, Gly-144 by Ser, Leu-288 by Met, and Pro-377 by Leu. Alignment of hydrophobic clusters also supported homologous folds (data not shown). Therefore, we sought to build a three-dimensional model of the entire protein based on the homology (Fig. 1) using Modeler (36). To find an accurate template, PDB was searched using the Blast algorithm. Horse leukocyte elastase inhibitor and α-antitrypsin both displaying over 30% identity with Iris (Fig. 2) were chosen as templates for the models corresponding to the cleaved state and uncleaved state, respectively (Fig. 1, *A* and *B*). Models were tested with Procheck, and all the residues were in the allowed regions of the Ramachandran plot.

The root mean square deviation (r.m.s.d.) between the uncleaved model (Fig. 1*A*) and its template is 0.44 Å (on 363 Cα). In contrast, the calculated r.m.s.d. between ovalbumin and α-antitrypsin is 1.57 Å.

We also compared the predicted RCL of Iris with the corresponding amino acid sequence of inhibitory and non-inhibitory serpins (Fig. 3). The RCL from Iris was aligned to the consensus RCL from inhibitory serpins (46), among these Glu-324, Gly-325, Thr-326, Ala-328, and Ala-332 were perfectly conserved. All conserved amino acids essential for the inhibitory function were present in Iris (Fig. 2). This alignment suggested that Iris has an inhibitory function based on the presence of methionine 340 adjacent to the cleavage site (position P1).

```
ATU    1  MPSSVSWGILLLAGLCCLVPVSLAEDPQGDAAQKTDTSHHDQDHPTFNKI   50
Iris   1  ------------------------------------------------MEASL    5
HLE    1  ------------------------------------------------ME-QL    4
                                                             ..
ATU   51  TPNLAEFAFSLYRQLAHQSNSTN--ILFSPVSIAAAFAMLSLGAKADTHD   98
Iris   6  SNHILNFSVDLYKQLKPSGKDTAGNVFCSPFSAAAALSMALAGARGNTAK   55
HLE    5  STANTHFAVDLFRALNES--DPTGNIFISPLSASSALAMIFAGTRGNTAA   52
          .    .* ..*.. *  .  .    .. **.*.  *. *. .* ...*

ATU   99  EILEGLNFNLTEIPE-AQIHEGFQELLRTLNQPDSQLQLTTGNGLFLSEG  147
Iris  56  QIAAILHS-----ND-DKIHDHFSNFLCKLPSYAPDVALHIANRMYSEQT   99
HLE   53  QVSKALYF-----DTVEDIHSRFQSLNADINKPGAPYILKLANRLYGEKT   97
          ..  .*        .  .**..*...  .. ..   . *. .*... ...

ATU  148  LKLVDKFLEDVKKLYHSEAFTVNFG-DTEEAKKQINDYVEKGTQGKIVDL  196
Iris 100  FHPKAEYTTLLQKSYDSTIKAVDFAGNADRVRLEVNAWVEEVTRSKIRDL  149
HLE   98  YNFLADFLASTQKMYGAELASVDFQQAPEDARKEINEWVKGQTEGKIPEL  147
          ...  ..    .* *. ..  *.*    .... ..* .*.. *..** .*

ATU  197  VK--ELDRDTVFALVNYIFFKGKWERPFEVKDTEEEDFHVDQVTTVKVPM  244
Iris 150  LAPGTVDSSTSLILVNAIYFKGLWDSQFKPSATKPGDFHLTPQTSKKVDM  199
HLE  148  LVKGMVDNMTKLVLVNAIYFKGNWQQKFMKEATRDAPFRLNKKDTKTVKM  197
          .    .*. * ..***.*.*** *.. *  . *.   *...  .. .* *
                          s3A
ATU  245  MKRLGMFNIQHCKKLSSWVLLMKYLGN-ATAIFFLPDEGK-----LQHLE  288
Iris 200  MHQEGDFKMGHCSDLKVTALEIPYKGNKTSMVILLPEDVE----GLSVLE  245
HLE  198  MYQKKKFPYNYIEDLKCRVLELPYQGKELSMIILLPDDIEDESTGLEKIE  247
          * . . * ..  ..*.  .* . * *.  .....**....     *. .*

ATU  289  NELTHDIITKFL--ENEDRRSAS-LHLPKLSITGTYDLKSVLGQLGITKV  335
Iris 246  EHLTAPKLSALL--GGMYATSDVNLRLPKFKLEQSIGLKDVLMAMGVKDF  293
HLE  248  KQLTLDKLREWTKPENLY-LAEVNVHLPRFKLEESYDLTSHLARLGVQDL  296
          ..**   .. .  ..          ..**.........*.. *. .*....

ATU  336  FS-NGADLSGVTEEAPLKLSKAVHKAVLTIDEKGTEAAGAMFLEAIPMSI  384
Iris 294  FT-SLADLSGISAAGNLCASDVIHKAFVEVNEEGTEAAAATAIPIMLMCA  342
HLE  297  FNRGKADLSGMSGARDLFVSKIIHKSFVDLNEEGTEAAAATAGTILLA--  344
          *. . *****..    * .*...** .....*.*****.* .. ....
                                                  RCL
ATU  385  PP----EVKFNKPFVFLMIEQNTKSPLFMGKVVNPTQK             418
Iris 343  RFPQVVNFFVDRPFMFLIHSHDPDVVLFMGSIREL---             377
HLE    -  ------------------------------------              -
```

FIGURE 2. **Alignment of Iris with α-antitrypsin and horse leukocyte elastase inhibitor.** Amino acid sequence alignment between α-antitrypsin (PDB code: 1ATU) from residue 46 to 418, Iris from residue 1 to 377, and horse leukocyte elastase inhibitor (PDB code: 1HLE) from residue 1 to 344. This alignment was obtained using the ClustalW algorithm. *Dots* indicate similar amino acids, and *stars* indicate identical amino acids. *Indents* indicate gaps. Conserved domains are *boxed*. The *open boxes* indicate the position of the RCL domain and the highly conserved serpin residues (s3a domain). The *shaded box* stands for the serpin signature (Prosite code: PS00284) in Iris.

Inhibitor																				
ATU	K	G	T	E	A	A	G	A	M	F	L	E	A	I	P	M	S	I	P	P
IRIS	E	G	T	E	A	A	A	A	T	A	I	P	I	M	L	M	C	A	R	F
HLEI	E	G	T	E	A	A	A	A	T	A	G	I	A	V	F	A	M	L	M	P
AlaSerpin A353K	E	G	A	E	A	A	A	A	N	A	F	G	I	V	P	K	S	L	I	L
Conserved residues	E/K/R	G	T/S		A/G/S			A/G/S												
Non-inhibitor																				
OVA	A	G	R	E	V	V	G	S	A	E	A	G	V	D	A	A	S	V	S	E
P notation	**16**	**15**	**14**	**13**	**12**	**11**	**10**	**9**	**8**	**7**	**6**	**5**	**4**	**3**	**2**	**1**				
interacting residues					x		x	x		x		x	x	x	x	x	x	x	x	x
																	cleavage site			

FIGURE 3. **Comparison of the RCL amino acid sequence in Iris and other inhibitory and non-inhibitory serpins.** Conserved residues critical for inhibitory activity have been identified by Hopkins *et al.* (45). *P notation* is from Schechter and Berger (33). *X* indicates a residue of Iris involved in the interaction with the protease, as deduced from the model of Iris in interaction with trypsin.

TABLE 1

Affinity constants and inhibition rate of proteases by rIris and its mutants

Proteases were incubated at an equimolar ratio with rIris or its mutants for 1 h at 37 °C. Residual activity in the presence of ovalbumin, a serpin with no inhibitory activity, is used as the 100% reference point (see "Materials and Methods"). The mutants A332P and L339A were not tested on proteases, which were not inhibited by rIris. Values are given as mean ± standard deviation of three repeats.

	Affinity constant		Inhibition			
	Iris for protease	M340R for protease	Iris for protease	M340R for protease	A332P for protease	L339A for protease
	k_a		%			
HLE	4.7 (±0.64).E6	ND[a]	70.3 (±4.68)	6.8 (±3.94)	13.5 (±4.68)	2.7 (±8.11)
PPE	2.2 (±0.15).E5	ND	74.5 (±7.32)	−2.4 (±5.52)	−4.2 (±4.88)	0.0 (±2.44)
t-Pa	2.9 (±0.15).E5	2.1 (±0.07).E4	30.8 (±7.69)	18.8 (±6.25)	2.6 (±4.44)	2.6 (±8.88)
Factor Xa	1.7 (±0.36).E5	1.4 (±0.25).E6	30.4 (±1.50)	68.5 (±3.15)	4.3 (±1.51)	1.7 (±1.51)
Thrombin	2.5 (±0.42).E4	1.3 (±0.45).E5	28.6 (±4.95)	61.8 (±4.95)	−5.7 (±4.95)	0.0 (±4.95)
Trypsin	1.5 (±0.42).E4	2.2 (±0.70).E7	11.8 (±1.86)	85.9 (±2.88)	2.5 (±1.04)	3.0 (±1.06)
Plasmin	ND	1.2 (±0.25).E5	1.7 (±7.64)	59.2 (±7.84)	ND	ND
Caspase 3	ND	ND	5.9 (±10.19)	5.0 (±7.86)	ND	ND
Papain	ND	ND	1.6 (±2.79)	3.0 (±2.51)	ND	ND
MMP12	ND	ND	−1.2 (±1.32)	−0.2 (±1.67)	ND	ND

[a] ND, not determined.

We further modeled and analyzed the interactions of Iris with trypsin to find the residues that make contact with the protease (Fig. 1*C*). The complex between trypsin and alaserpin (PDB code: 1K9O) was used as a template for this model. The r.m.s.d. between alaserpin and Iris is 0.22 Å. Using the Pex algorithm, we determined the residues involved in the interaction. Most of the important residues were located in the RCL, some specifically in the Hinge region (Fig. 3).

rIris Expression and Purification—The coding sequence of Iris was cloned in the vector pBlueBac4.5-V5-His (Invitrogen) in-frame with the V5-His tag, expressed in a baculovirus system and purified to homogeneity as confirmed by SDS-PAGE (data not shown). Affinity-purified rIris migrated at an apparent mass of 48 kDa on a 10% SDS-polyacrylamide gel (data not shown). This contrasted with an expected molecular weight of 44 kDa and suggested putative posttranslational modifications.

Inhibition of Protease Activity by rIris—We tested the ability of purified rIris to inhibit various serine proteases derived from human blood (leukocyte elastase, t-PA, factor Xa, plasmin, thrombin, and trypsin) or from porcine pancreas (pancreatic elastase), as well as two human cysteine proteases (caspase-3 and papain), and one human metalloelastase (MMP12). Recombinant Iris was incubated for 1 h at 37 °C with the various proteases, and the residual proteolytic activity was measured using synthetic chromogenic substrates. Most of the serine proteases were inhibited by rIris, as opposed to the two cysteine proteases and the metalloelastase, which did not show any significant drop of activity in presence of rIris (Table 1). From these data, the serine proteases could be distributed into three groups: (i) human leukocyte elastase and porcine pancreas elastase with a residual activity of ~30%; (ii) thrombin, t-PA, and factor Xa with a residual activity near 70%; and (iii) plasmin with 100% residual activity (no inhibitory effect of rIris).

To assess the binding kinetics, Iris and the different proteases were allowed to react together either directly in the presence of the substrate or for shorter variable periods of time before addition of the substrate. As shown in Fig. 4, the kinetics and the residual activities observed at the end of the kinetics are in agreement with the values observed after 1 h (Table 1). The data allow determination of the affinity rate constants for the interaction between rIris and the inhibited proteases. HLE was the most rapidly inhibited with a rate constant (k_a = 4.3 (±0.64) × 10^6), ~20 times faster than the pancreatic elastase (k_a = 2.1 (±0.15) × 10^5). Tissue plasminogen activator and factor Xa were inhibited with an association rate similar to that of pancreatic elastase; however, only 30% was inhibited as compared with 60% for the two elastases. Taken together, these results strongly suggest that rIris is a specific serine protease inhibitor and that its natural target proteases are leukocyte elastase and elastase-like serine proteases.

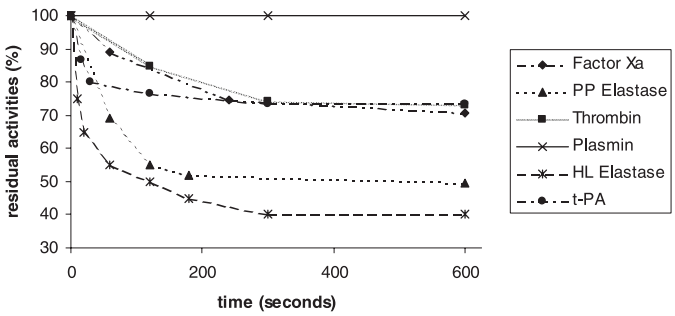

FIGURE 4. **Inhibition of proteases by Iris as function of the incubation time.** Proteases were incubated at equimolar ratio with rIris for variable periods of time as indicated on the *x*-axis before addition of substrate (0.5 mM). Residual activities indicated by the amount of metabolized substrate are reported on the *y*-axis. They were measured as absorbance values at 405 nm.

Mutants of rIris—Based on the putative three-dimensional structure of Iris, positions near or in the RCL domain that should affect the inhibitory function of Iris were predicted. Three positions were selected for mutagenesis (Fig. 2). The first is Ala-332 at P9 in the hinge domain mutated to proline. This mutation was predicted to disrupt the interaction of Iris with the protease, render the hinge more rigid, and ultimately hinder the insertion of the RCL into β-sheet A. The second mutant was generated by changing Leu-339 (amino acid P2 in the interaction domain) to an alanine. This mutation was predicted to modify the hydrophobicity and the steric hindrance at that position in an attempt to alter the interaction with the protease. These two mutants were named A332P and L339A, respectively. Both mutants were produced in the baculovirus expression system and purified as efficiently as the wild-type protein. *In vitro* enzymatic assays indicated that these two mutants completely lost their ability to inhibit any tested protease except for a weak activity of A332P against HLE (Table 1). These data strongly suggest that the mechanism of rIris activity

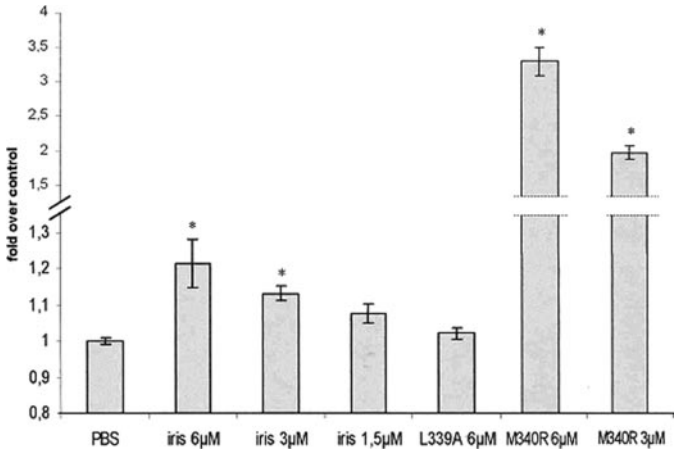

FIGURE 5. **Iris inhibits the contact phase coagulation pathway.** Contact phase-activated coagulation time in the presence of rIris wild-type or mutant M340R. Values are given as -fold increase compared with the HBSS control as indicated on the *x*-axis. Mutant L339A lost the anti-protease activity due to a mutation in the RCL. Clotting time is defined after activation with prothrombin time. ANOVA repeated measures was used, $p = 0.008$. *, $p < 0.05$ *versus* phosphate-buffered saline, Dunnett's post hoc test.

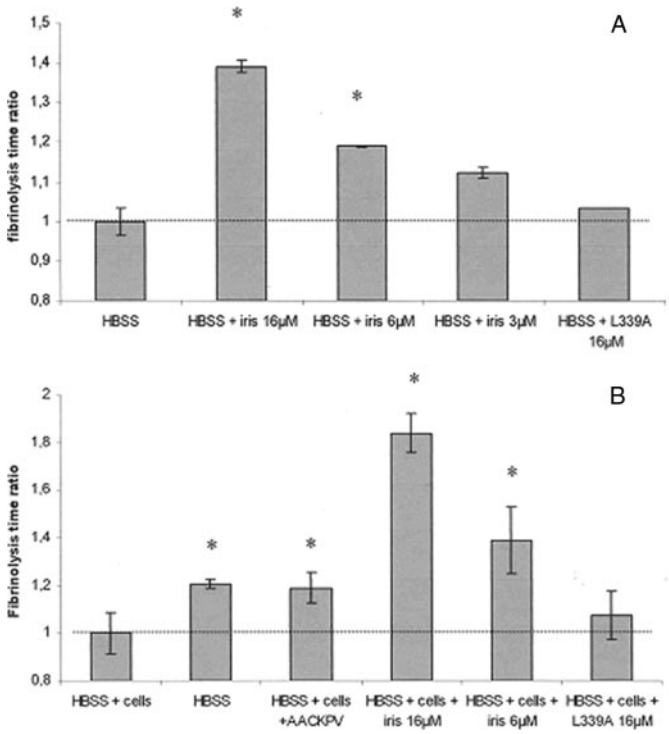

FIGURE 6. **Iris inhibits fibrinolysis.** ECLT increased with rIris concentration. *A*, euglobulin fraction was resuspended in HBSS in the presence of Iris wild type or mutant at the indicated concentrations. Values are given as the -fold increase of clot lysis time compared with the HBSS control. Mutant L339A lost the anti-protease activity due to a mutation in the RCL. ANOVA repeated measures was used, $p = 0.006$. *, $p < 0.05$ *versus* HBSS, Bonferroni post hoc test. *B*, euglobulin fraction was resuspended in HBSS in the presence of different concentrations of rIris wild type or mutants. White blood cells (86% neutrophils) were added to a final concentration of 5×10^6 cells/ml. Values are given as the -fold increase compared with *HBSS + cells* control. *AACKPV* is a specific inhibitor of leukocyte elastase. Mutant L339A lost the anti-protease activity due to a mutation in the RCL. Values for M340R could not be presented because the experiment was stopped after 72 h while still no fibrinolysis could be observed. ANOVA repeated measures was used, $p < 0.001$. *, $p < 0.05$ *versus* HBSS, Dunnett's post hoc test.

is of the serpin type. This hypothesis is supported by the presence of a methionine (Met-340) at the P1 position. To further test this possibility, this residue was changed to an arginine. According to Owen *et al.* (47, 48), this mutation should change the affinity of Iris for other serine proteases. *In vitro* enzymatic assays showed that mutant M340R lost its ability to inhibit both human leukocyte and pig pancreatic elastases. More strikingly this mutant had a much stronger affinity than the wild-type Iris for factor Xa ($k_a = 1.4\ (\pm 0.25) \times 10^6$ *versus* $1.7\ (\pm 0.36) \times 10^5$), thrombin ($k_a = 1.3\ (\pm 0.45) \times 10^5$ *versus* $2.5\ (\pm 0.42) \times 10^4$), and trypsin ($k_a = 2.2\ (\pm 0.70) \times 10^7$ *versus* $1.5\ (\pm 0.42) \times 10^4$) (see Table 1). This correlated with an increased inhibitory activity for these proteases. In addition, the mutant M340R remarkably inhibited plasmin. Finally, we did not observe any change of activity against the two cysteine proteases and the metalloprotease.

rIris Inhibits the Contact Phase-activated Coagulation Pathway—Several serine proteases inhibited by Iris are involved in coagulation. We therefore investigated the effect of rIris on blood clotting using assays that measure the contact phase- and the tissue factor-activated coagulation pathways. An assay designed to monitor the extrinsic coagulation (tissue factor-activated) detected only a slight increase of the clotting time upon addition of rIris (6% for 6 μM final of rIris). On the contrary it significantly increased the intrinsic coagulation time in a dose-dependent manner (Fig. 5). Indeed, addition of 6 μM rIris prolonged the intrinsic (contact phase) coagulation time by 21%. On the other hand, the M340R mutant was active in both assays, causing a drastic increase of both intrinsic and extrinsic coagulation times by 250% (data not shown) and 300% (Fig. 5), respectively. Finally, mutant L339A lost all activity as its addition at the same concentration had no effect at all.

rIris Inhibits Fibrinolysis—The ECLT assay was used to determine the effect of rIris on fibrinolysis. As shown on Fig. 6, rIris extended the fibrinolysis time in a dose-dependent manner. The presence of rIris (16 μM) extended fibrinolysis time up to 39% as compared with the HBSS control (Fig. 6*A*). We further tested the effect of rIris on euglobulin in the presence of added human leukocytes. As expected, leukocytes decreased fibrinolysis time (~20%) likely due to the release of elastase by neutrophils. In this cellular setting, rIris increased fibrinolysis time by 83 ± 6.3% (Fig. 6*B*) as opposed to the addition of 16 μM mutant L339A, which had no effect on fibrinolysis time, regardless of the addition of neutrophils (Fig. 6, *A* and *B*). Moreover, addition of 16 μM mutant M340R completely inhibited fibrinolysis (data not shown). This effect was drastic, as no fibrinolysis could be detected as long as 72 h after the beginning of the assay, whereas regular fibrinolysis time was ~6 h. Finally, to determine if this increase was due to an interaction of Iris on the cell surface, cells were preincubated for 1 h in the presence of rIris, washed, and tested in the ECLT assay. In this case, we did not observe any increase of the fibrinolysis time (data not shown).

rIris Inhibits Primary Hemostasis—Closure time was measured with PFA-100, as a reliable indication of the platelet adhesion time. rIris delayed closure time in a dose-dependent manner in four out of the five samples from five healthy adults, although for one sample, rIris had no effect (Fig. 7). The addition of 2 μM rIris (final concentration) increased platelet adhesion time by 15–30%, an effect also observed with mutants L339A and M340R.

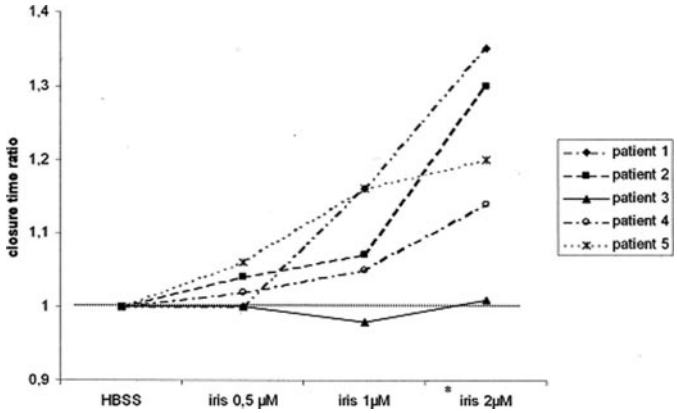

FIGURE 7. **Iris increases platelet adhesion time.** Platelet adhesion time increased with rIris concentration. Blood samples were collected from five healthy volunteers into 0.13 M citrated vacuum tubes. Platelet adhesion times were measured through the closure time ratio with PFA-100® (Dade, Behring). Samples were 1/10 protein in HBSS and 9/10 anti-coagulated whole citrated blood. Values are given as the -fold increase compared with the HBSS control. The time required to obtain full occlusion of the aperture is defined as the collagen/epinephrine closure time. ANOVA repeated measures was used, $p = 0.001$. *, $p < 0.05$ *versus* control, Bonferroni post hoc test.

DISCUSSION

The modulation of hemostasis by tick saliva is of major importance in the successful accomplishment of the blood meal (2, 3). Although extensive information is available about the effects of tick feeding on host blood coagulation, little is known about the nature of the active factors expressed by tick salivary glands. Nevertheless, a few anti-hemostatic compounds have been molecularly characterized in both soft and hard ticks, including a platelet βIIbα3 integrin antagonist and inhibitors of blood coagulation (7–16).

In this work, we have characterized the anti-hemostatic properties of a protein induced during the tick feeding process, which was formerly named Iris for "*I. ricinus* immunosuppressor" due to its immunomodulatory properties (35). Amino acid sequence comparisons showed that Iris is highly homologous to the pig leukocyte elastase inhibitor (35). In addition, the high conservation of amino acid patterns (see Figs. 2 and 3) as well as the presence of the serpin signature (Prosite code: PS00284) reactive center loop confirm that Iris is a member of the serpin superfamily (45). The homology with α-antitrypsin and horse leukocyte elastase inhibitor allowed us to construct a three-dimensional model of the entire protein. These studies also support the notion that Iris belongs to the serpin superfamily with inhibitory function.

Inhibitory serpins are expressed in a cell-specific manner and are involved in a wide variety of fundamental biological processes such as blood coagulation, complement activation, fibrinolysis, angiogenesis, inflammation, and tumor suppression (23–25). Therefore, Iris was expressed as a recombinant protein and purified to near homogeneity to examine its properties as an inhibitor of blood coagulation, fibrinolysis, and primary hemostasis. rIris inhibited serine proteases (HLE, t-PA, thrombin, and factor Xa) involved in these mechanisms (Table 1). Affinity rate constants and inhibition values demonstrated that, among these targets, rIris has the highest affinity for human leukocyte elastase (Fig. 4 and Table 1) as predicted by the structural studies. These values are very similar to those published for α1-antitrypsin (49, 50) suggesting that Iris is an α1-antitrypsin-like inhibitor. These results also suggest that elastase-like proteases are the likely natural targets of Iris.

It is well documented that the inhibitory activity of serpins is mediated by the RCL domain. This was confirmed by our structural model, which predicted the interaction between Iris and serine proteases through the RCL motif. We therefore constructed mutants that should alter the RCL motif and could affect either the anti-proteolytic specificity or the inhibitory activity of Iris. Thus, we generated one mutant (M340R, located at position P1 of the RCL domain) to see whether the specificity changes from elastase to factor Xa and thrombin as predicted. Relative to Iris, mutant M340R had a 10-fold higher affinity for factor Xa and thrombin, and ~1,000-fold higher affinity for trypsin. Concomitantly, mutant M340R lost its ability to inhibit human or pig elastases. Moreover, it gained inhibitory activity against plasmin. Therefore, mutation of Met-340 into an arginine residue changed our "α1-antitrypsin like" to an "antithrombin-like" protein as observed for Pittsburgh factor α1-antitrypsin (47, 48). We also introduced two point mutations (A332P and L339A) in the hinge region (position P9) and in the RCL domain (position P2), respectively, predicted to invalidate the protein. In particular, mutant A332P was predicted to have an altered interaction with the protease as a result of the stereochemical constraints imposed by the proline ring. It should render the hinge region more rigid and prevent the insertion of the RCL domain into β-sheet A. As a result, the reaction should proceed directly to the cleaved product (release of the RCL domain), and there should be no inhibition of the protease. Both mutants lost anti-proteolytic activity specific to serine proteases. We therefore propose that the mechanism of inhibition of Iris on elastase-like proteases is the "suicidal" type that involves deformation of the protease and not just a "lock of the active site" type, as for the traditional inhibitors. Because none of these inactive mutants exhibited any inhibitory activity, we subsequently used only L339A to characterize the mode of action of Iris in experimental hemostatic systems.

Numerous serine proteases are involved in blood coagulation pathways. *In vitro* enzymatic assays showed that Iris inhibited several of these proteases (*e.g.* factor Xa or thrombin) suggesting that Iris could act as an inhibitor of coagulation. While monitoring the tissue factor-activated pathway, we did not observe a significant modification of clotting time by adding rIris in the presence or absence of THP1 monocytes (data not shown). However, the contact phase-activated coagulation time was significantly increased in a dose-dependent manner by the addition of rIris, whereas mutant L339A lost this effect. There is therefore a correlation between the anti-protease activity and an effect on coagulation. The preferred inhibition of the contact phase-activated pathway over the tissue factor-activated pathway by rIris is consistent with the current knowledge of the biochemistry of the two pathways. Indeed, the former is composed mainly of serine proteases such as factors IXa and XIIa that could be the target of inhibitory serpins while the tissue factor pathway is naturally inhibited by a kunitz protein (9) rather than a serpin. However, despite the fact that Iris inhibited significantly the contact phase-activated coagulation pathway time, it appeared that Iris was not a powerful antico-

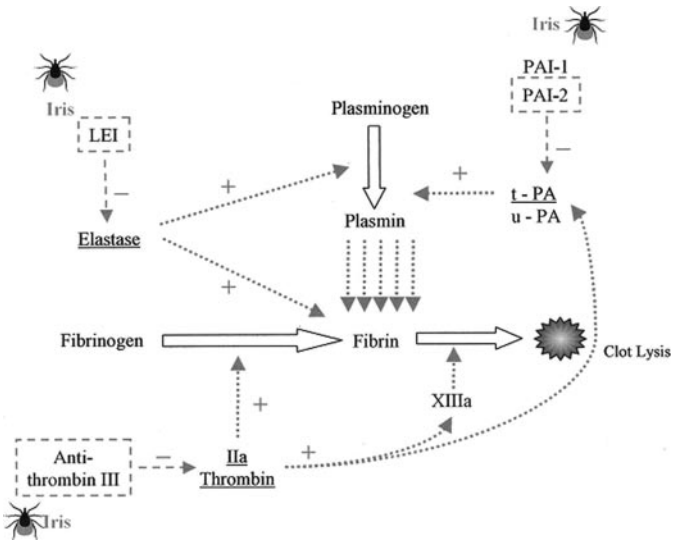

FIGURE 8. **A model describing the putative inhibitory actions of iris on fibrinolysis.** The fibrin clot is formed by the processing action of thrombin on fibrinogen. As soon as the presence of fibrin is detected, the plasminogen is processed and activated into plasmin by the action of t-Pa. The plasmin then degrades the fibrin clot. In addition, elastase also plays a role in the degradation of the fibrin clot. The majority of the factors implied in the fibrinolysis are controlled by serpins. *Dotted arrows* represent activation by a molecule, *dashed arrows* represent inhibition, and *open arrows* were used to represent activation of a protein. Serine proteases inhibited by rIris are *underlined*. Iris homologs are *framed*. *PAI*, plasminogen activator inhibitor; *u-PA*, urokinase plasminogen activator; *LEI*, leukocyte elastase inhibitor. *IIa* and *XIIIa* correspond to activated factors II and XIII, respectively.

agulant. The mutant M340R that we generated, on the contrary, acts like a powerful inhibitor of coagulation. This mutant, while displaying no affinity and loosing completely its inhibitory activity to elastases, gained inhibitory activity against factor Xa and thrombin according to an increase of its affinity constant to these proteases. Therefore, comparing to the blood coagulation inhibitory properties of Iris, the mutant M340R shows an increased inhibitory potential of the surface-activated coagulation pathway and exhibits new inhibitory activity on the tissue factor pathway.

Lysis of the fibrin clot also involves several serine proteases, including plasmin, t-PA, or leukocyte elastase. The calculation of association second order rates and percentages of inhibition showed that the t-PA and leukocyte elastase are targets of rIris. This is consistent with the high degree of sequence identity of Iris with the human leukocyte elastase inhibitor and with plasminogen activator inhibitor type 2. The role of rIris on fibrinolysis was therefore evaluated by using the ECLT assay. To ensure that the increase of fibrinolysis time was not an artifact due to inhibition of fibrino-formation, the ECLT assay was performed in the presence of a large excess of thrombin. In these conditions, rIris only inhibited t-PA (Fig. 8). This inhibition slowed the plasminogen activation and consequently increased the fibrinolysis time (Fig. 6*A*). We further tested the effect of rIris on plasma in the presence of human leukocytes (Fig. 6*B*). As expected, leukocytes decreased fibrinolysis time by 20%, probably due to their secretion of elastase. In that situation, the action of rIris was accordingly underlined prolonging the fibrinolysis time by ~83%, dramatically exceeding the values obtained in the absence of neutrophils. In addition, mutant L339A had no effect on fibrinolysis time whether in presence or absence of neutrophils. Taken together, these results strongly suggest that rIris inhibits fibrinolysis due to its anti-proteolysis activity via the RCL motif. They indicate that this activity is mediated by inhibition both of t-PA and the elastase released by leukocytes (Fig. 8). Finally, M340R increased dramatically its ability to counteract fibrinolysis, an effect related to a change of the target. Thus, while M340R lost its activity to t-PA and elastase, it gained activity on plasmin.

We also examined the action of rIris on primary hemostasis. rIris and both RCL mutants (L339A and M340R) promote a dose-dependent increase of the PFA closure time, a reliable measure of the platelet adhesion time (Fig. 8). This is in contrast with the observed effect of rIris on blood coagulation and fibrinolysis, an activity that is indeed lost in the RCL mutants. Because an intact RCL seems dispensable for iris action on primary hemostasis, this could be explained by the presence of exosites (predicted by the receptor binding domain method (51)) that could be involved in an interaction with other proteins such as the von Willebrand factor and βIIbα3 integrin. These proteins are indeed required for platelet adhesion to components of the vessel wall via domains (52) that interact with specific regions of proteins located on endothelial cells. Therefore, Iris could inhibit primary hemostasis by interacting with proteins involved in such a mechanism.

We have previously shown that Iris inhibits the secretion of pro-inflammatory cytokines and suppresses the TH1 host response (35). We now report that Iris acts as an anticoagulant and a hypo-fibrinolytic factor by targeting serine proteases, especially elastase-like proteins. In addition, Iris seems to hinder platelet adhesion via a mechanism independent of its enzyme inhibitory activity. Interestingly, the involvement of Iris in modulation of both the hemostatic and immune systems is consistent with those modulations caused by tick saliva and tick salivary gland extracts (2–6).

Blood coagulation and fibrinolysis are powerful barriers to blood feeding by hematophagous parasites (53). Thus, it is not surprising to find proteins in tick saliva that are able to inhibit these two processes. Among key players in these, leukocyte elastase is possibly detrimental to different steps of the ticks' blood meal through (i) activation of plasminogen into plasmin, (ii) hydrolysis of fibrin clots, (iii) activation of a pro-inflammatory response (54, 55), and (iv) digestion of the extracellular matrix and destruction of tick's gut tissues.

Hence, inhibitors of elastase, such as Iris could play a major role in blood feeding through interference with these processes. More precisely, it (i) inhibits fibrinolysis, (ii) could prevent the rejection of the parasites by the host, and (iii) helps to prevent the disanchoring of tick mouthparts before the end of feeding or disaggregation of midgut tissues during ingestion of blood. The expression of Iris is up-regulated during the blood meal with a maximum at day 4 (18), which is precisely the time when the *I. ricinus* female starts to swallow the highest amount of blood (1, 56). At this step, Iris could both be introduced to the midgut along with the blood meal and be an important tick countermeasure to a variety of defense mechanisms developed by the host.

In conclusion, we have analyzed the anti-hemostatic properties of a serine protease inhibitor, which could play a major role in the completion of the blood meal of ticks. The results indicate that, in addition to being an anti-inflammatory factor and a modulator of the host immune response (35), Iris is a key factor in the modulation of host local hemostasis. To our knowledge, this is the first ectoparasite serpin that alters aspects of both hemostasis and the immune system. In the near future, we will investigate the involvement of Iris in the physiology of *I. ricinus* during the blood meal and to assess its suitability as a candidate for tick vaccine development.

Acknowledgments—We thank Valérie Denis, Virginie Blasioli, and scientists from the Henogen Company for their invaluable technical assistance and scientific help. We are also thankful to Dr. Bernard Couvreur (Institute of Molecular Biology and Medecine, Université Libre de Bruxelles, Brussels, Belgium) for critical reading of the manuscript.

REFERENCES

1. Sauer, J. R., McSwain, J. L., Bowman, A. S., and Essenberg, R. C. (1995) *Annu. Rev. Entomol.* **40,** 245–267
2. Champagne, D. E. (2004) *Curr. Drug Targets* **4,** 375–396
3. Ribeiro, J. M. (1995) *Infect Agents Dis.* **4,** 143–152
4. Kopecky, J., and Kuthejlova, M. (1998) *Parasite Immunol.* **20,** 169–174
5. Wikel, S. K. (1996) *Annu. Rev. Parasitol.* **84,** 304–309
6. Brossard, M., and Wikel, S. K. (2004) *Parasitology* **129,** 161–176
7. Hoffmann, A., Walsmann, P., Riesener, G., Paintz, M., and Markwardt, F. (1991) *Pharmazie.* **46,** 209–212
8. Horn, F., dos Santos, P. C., and Termignoni C. (2000) *Arch. Biochem. Biophys.* **384,** 68–73
9. Francischetti, I. M., Valenzuela, J. G., Andersen, J. F., Mather, T. N., and Ribeiro, J. M. (2002) *Blood* **99,** 3602–3612
10. Lai, R., Takeuchi, H., Jonczy, J., Rees, H. H., and Turner, P. C. (2004) *Gene* (*Amst.*) **342,** 243–249
11. Law, J. H., Ribeiro, J. M., and Wells, M. A. (1992) *Annu. Rev. Biochem.* **61,** 87–111
12. Iwanaga, S., Okada, M., Isawa, H., Morita, A., Yuda, M., and Chinzei, Y. (2003) *Eur. J. Biochem.* **270,** 1926–1934
13. Waxman, L., Smith, D. E., Arcuri, K. E., and Vlasuk, G. P. (1990) *Science* **248,** 593–596
14. Sangamnatdej, S., Paesen, G. C., Slovak, M., and Nuttall, P. A. (2002) *Insect. Mol. Biol.* **11,** 79–86
15. Valenzuela, J. G., Charlab, R., Mather, T. N., and Ribeiro, J. M. (2000) *J. Biol. Chem.* **275,** 18717–18723
16. Ribeiro, J. M. (1987) *Exp. Parasitol.* **64,** 347–353
17. Das, S., Banerjee, G., DePonte, K., Marcantonio, N., Kantor, F. S., and Fikrig, E. (2001) *J. Infect. Dis.* **184,** 1056–1064
18. Leboulle, G., Rochez, C., Louahed, J., Ruti, B., Brossard, M., Bollen, A., and Godfroid, E. (2002) *Am. J. Trop. Med. Hyg.* **66,** 225–233
19. Valenzuela, J. G., Francischetti, I. M., Pham, V. M., Garfield, M. K., Mather, T. N., and Ribeiro, J. M. (2002) *J. Exp. Biol.* **205,** 2843–2864
20. Ribeiro, J. M., Alarcon-Chaidez, F., Francischetti, I. M., Mans, B. J., Mather, T. N., Valenzuela, J. G., and Wikel, S. K. (2006) *Insect Biochem. Mol. Biol.* **36,** 111–129
21. Kanost, M. R. (1999) *Dev. Comp. Immunol.* **23,** 291–301
22. Van Gent, D., Sharp, P., Morgan, K., and Kalsheker, N. (2003) *J. Biochem. Cell Biol.* **35,** 1536–1547
23. Davie, E. W., Fujikawa, K., and Kisiel, W. (1991) *Biochemistry* **30,** 10363–10370
24. Hekman, C. M., and Loskutoff, D. J. (1987) *Semin. Thromb. Hemost.* **13,** 514–527
25. Rubin, H. (1996) *Nat. Med.* **2,** 632–633
26. Silverman, G. A., Bird, P. I., Carrell, R. W., Church, F. C., Coughlin, P. B., Gettins, P. G., Irving, J. A., Lomas, D. A., Luke, C. J., Moyer, R. W., Pemberton, P. A., Remold-O'Donnell, E., Salvesen, G. S., Travis, J., and Whisstock, J. C. (2001) *J. Biol. Chem.* **276,** 33293–33296
27. Imamura, S., da Silva Vaz Junior, I., Sugino, M., Ohashi, K., and Onuma, M. (2005) *Vaccine* **23,** 1301–1311
28. Kazimirova, M., Jancinova, V., Petrikova, M., Takac, P., Labuda, M., and Nosal, R. (2002) *Exp. Appl. Acarol.* **28,** 97–105
29. Mulenga, A., Tsuda, A., Onuma, M., and Sugimoto, C. (2003) *Insect. Biochem. Mol. Biol.* **33,** 267–276
30. Sugino, M., Imamura, S., Mulenga, A., Nakajima, M., Tsuda, A., Ohashi, K., and Onuma, M. (2003) *Vaccine* **21,** 2844–2851
31. Mulenga, A., Sugino, M., Nakajim, M., Sugimoto, C., and Onuma, M. (2001) *J. Vet. Med. Sci.* **63,** 1063–1069
32. Mulenga, A., Sugimoto, C., and Onuma, M. (2000) *Microbes Infect.* **2,** 1353–1361
33. Schechter, I., and Berger, A. (1967) *Biochem. Biophys. Res. Commun.* **27,** 157–162
34. Narasimhan, S., Montgomery, R. R., DePonte, K., Tschudi, C., Marcantonio, N., Anderson, J. F., Sauer, J. R., Cappello, M., Kantor, F. S., and Fikrig, E. (2004) *Proc. Natl. Acad. Sci. U. S. A.* **3,** 1141–1146
35. Leboulle, G., Crippa, M., Decrem, Y., Mejri, N., Brossard, M., Bollen, A., and Godfroid, E. (2002) *J. Biol. Chem.* **277,** 10083–10089
36. Sali, A., and Blundell, T. L. (1993) *J. Mol. Biol.* **234,** 779–815
37. Gaboriaud, C., Bissery, V., Benchetrit, T., and Mornon, J. P. (1987) *FEBS Lett.* **224,** 149–155
38. Laskowski, R. A., MacArthur, M. W., Moss, D. S., and Thornton, J. M. (1993) *J. Appl. Crystallogr.* **26,** 283–291
39. Rahman, M., and Brasseur, R. (1994) *J. Mol. Graph.* **12,** 212–218
40. Schwede, T., Kopp, J., Guex, N., and Peitsch, M. C. (2003) *Nucleic Acids Res.* **31,** 3391–3395
41. Thomas, A., Bouffioux, O., Geeurickx, D., and Brasseur, R. (2001) *Proteins Struct. Funct. Genet.* **43,** 28–36
42. Frommherz, K. J., Faller, B., and Bieth, J. G. (1991) *J. Biol. Chem.* **266,** 15356–15362
43. Zouaoui Boudjeltia, K., Cauchie, P., Remacle, C., Guillaume, M., Brohee, D., Hubert, J. L., and Vanhaeverbeek, M. (2002) *BMC Biotech.* **2,** 8
44. Kundu, S. K., Heilmann, E. J., Sio, R., Garcia, C., Davidson, R. M., and Ostgaard, R. A. (1995) *Semin. Thromb. Hemost.* **21,** 106–112.
45. Irving, J. A., Pike, R. N., Lesk, A. M., and Whisstock, J. C. (2000) *Genome Res.* **10,** 1845–1864
46. Hopkins, P. C., Carrell, R. W., and Stone, S. R. (1993) *Biochemistry* **32,** 7650–7657
47. Travis, J., Matheson, N. R., George, P. M., and Carrell, R. W. (1986) *Biol. Chem. Hoppe-Seyler* **367,** 853–859
48. Owen, M. C., Brennan, S. O., Lewis, J. H., and Carrell, R. W. (1983) *N. Engl. J. Med.* **309,** 694–698
49. Beatty, K., Bieth, J. G., and Travis, J. (1980) *Biol. Chem.* **255,** 3931–3934
50. Ellis, V., Scully, M., MacGregor, I., and Kakkar, V. (1982) *Biochim. Biophys. Acta* **701,** 24–31
51. Gallet, X., Charloteaux, B., Thomas, A., and Brasseur, R. (2000) *J. Mol. Biol.* **302,** 917–926
52. Caen, J. P., and Levy-Toledano, S. (1973) *Nat. New. Biol.* **244,** 159–160
53. Doolittle, R. F., and Feng, D. F. (1987) *Cold Spring Harbor Symp. Quant. Biol.* **52,** 869–874
54. Shepherd, J. C., Aitken, A., and McManus, D. P. (1991) *Mol. Biochem. Parasitol.* **44,** 81–90
55. Maizels, R. M., Gomez-Escobar, N., Gregory, W. F., Murray, J., and Zang, X. (2001) *Int. J. Parasitol.* **31,** 889–898
56. Sonenshine, D. E. (1991) *Biology of Ticks*, Vol. 1, Oxford University Press, New York, pp. 95–97